

An approach to accurately identifying binders in historic mortars by the combination of microscopic and microanalytical techniques

Luís Almeida ^{1,*}, António Santos Silva ², Rosário Veiga ³ and José Mirão ⁴

¹ HERCULES Laboratory, University of Évora, Largo Marquês de Marialva, 8, 7000-809 Évora, Portugal; UNI-ARQ, Archaeology Center of the University of Lisbon, Alameda da Universidade, Faculty of Letters, 1600-214 Lisbon, Portugal; lfalmeida@uevora.pt

² LNEC, National Laboratory for Civil Engineering, Materials Department, Av. do Brasil, 101, 1700-066 Lisbon, Portugal; ssilva@lnec.pt

³ LNEC, National Laboratory for Civil Engineering, Buildings Department, Av. do Brasil, 101, 1700-066 Lisbon, Portugal; rveiga@lnec.pt

⁴ HERCULES Laboratory, University of Évora, Largo Marquês de Marialva, 8, 7000-809 Évora, Portugal; Geosciences Department, University of Évora, Colégio Luís António Verney, Rua Romão Ramalho, nº 59, 7000-671 Évora, Portugal; jmirao@uevora.pt

* Correspondence: lfalmeida@uevora.pt

Abstract: Mortars are among the most important materials in building construction. They are generally obtained by the mix of aggregates with an inorganic binder. The identification of mortar constituents, particularly the binder type in historic buildings, is one of the essential aspects of building conservation, considering that the new conservation materials must be chemically, mechanically, and physically compatible with the old masonries. Among other techniques used to characterise binders, those related to optical and electronic microscopy are particularly important. Microscopy and combined techniques may be the key to this identification since the classic mineralogical and chemical-based identification approaches are not conclusive enough in investigating the types of hydraulic binders in mortars. This work presents an analysis procedure to identify mortar binders by combining EDS microanalysis and petrography. Mortar samples of known composition were used as a reference for analysing mortars from historic buildings. The proposed methodology made it possible to identify the type of binder or a mixture of binders based on the identification of the binder features by petrography together with analysis of the chemical composition of the paste by X-ray microanalysis under a scanning electron microscope.

Keywords: Petrography; SEM-EDS; mortars; binders; characterisation

Citation: To be added by editorial staff during production.

Academic Editor: Firstname Last-name

Received: date

Revised: date

Accepted: date

Published: date



Copyright: © 2024 by the authors. Submitted for possible open access publication under the terms and conditions of the Creative Commons Attribution (CC BY) license (<https://creativecommons.org/licenses/by/4.0/>).

1. Introduction

Mortars are an essential part of the construction of built structures and have become more sophisticated over time, evolving in close connection with manufacturing technologies and construction techniques.

Mortars have various functions, such as rendering walls, repointing and joints, covering and bedding masonry elements or bonding ceramic tiles.

Over time, the functions assigned to mortars have mostly stayed the same. They are generally composite materials technologically characterised by a mixture of aggregates with one or more types of binders, water, and additions. The most typical traditional binders could be based on clay, lime, and gypsum [1,2]. The innovative changes were related to the binders' production technology, the mix's formulation, and the incorporation of different materials that granted characteristics or performances that increased durability

and strength. Regarding innovation in formulation, pozzolanic materials in Roman times stand out, namely replacing volcanic ashes with crushed or powdered ceramic fragments when the former was unavailable [3].

There have been considerable changes throughout history in the manufacture of binders, especially since the 18th century, when technologies were discovered that made it possible to produce various types of hydraulic binders and expand the application of hydraulic mortars in construction.

Lime mortars can be divided into air lime mortars and hydraulic lime mortars, depending on whether air or hydraulic lime is used. Compounds can also be incorporated to make mortars hydraulic (e.g., natural or artificial pozzolans, crushed bricks, silica, and amorphous alumina) even without a hydraulic binder.

Hydraulic mortars can also be based on natural or artificial types of cement, such as Portland cement. Hydraulic lime is obtained from a burnt natural rock (siliceous/argillaceous limestone or calcareous marl) below the sintering temperature (800–1200 °C). It must contain enough free CaO to be slaked with water and capable of setting under water. The calcined product must contain a minimum amount of free CaO to reduce the entire mass to a powder when slaked [1].

Natural cement, also known as Roman cement, was patented by James Parker in England in 1796 [4]; its hydraulicity is due to the raw material used. Despite implied links to the Roman binders, Parker's 'Roman cement' was a proper hydraulic cement very different from the hydraulic binders used by the Romans in which pozzolanic materials, not cementitious in themselves, had combined with lime in the presence of water to form insoluble compounds possessing cementing properties [5].

The standardisation of technological processes has led to the manufacture of various types of binders with characteristics that are now known in more recent historical periods. Air lime can currently be classified according to standard EN 459-1:2015 [6], which divides lime into calcium (CL) or dolomitic (DL), considering its chemical composition. The same standard also establishes the classification of natural hydraulic lime (NHL), which differs chemically and mineralogically, leading to different compressive strength ranges.

Air lime is divided into fat and lean. Fat air lime is derived from almost pure limestone with at least 99% carbonate content. Lean (generally greyish) is derived from limestones with clay and other impurity contents between 1 and 5% [7].

Roman cement is a type of cement made from marl or septaria that contains 25% or more clay. This cement is considered "natural" because all the necessary components, such as lime, silica, and alumina, are found in a single source material, unlike Portland cement, which is made from different sources [8].

Although they are natural hydraulic binders, according to Kozłowski (2010) [5], natural cements are distinct from hydraulic limes in that they have low levels of free lime, which means they need to be ground instead of slaked. They are also different from Portland cements due to their different chemical composition, resulting in significantly lower calcination temperatures. The primary hydraulic phase in natural cements is C₂S (dicalcium silicate or belite), whereas in ordinary Portland cement, it is C₃S (tricalcium silicate or alite).

Although both Roman cement and natural hydraulic lime are calcined at low temperatures, they differ in that the cement hardens quickly, usually in less than 15 min. Both materials contain substantial amounts of belite and have a prolonged strength development profile. Roman cements can be differentiated from Portland cements by the presence of residual quartz and calcite and the absence, or residual content, of tricalcium silicate (C₃S - alite), which is responsible for the substantial strength development in Portland cements [8].

Historical cementitious or highly hydraulic mortar binders exhibit a lesser degree of chemical definition than their contemporary counterparts. Consequently, comprehensive characterisation of these binders within mortar specimens requires meticulous examination of the residual unhydrated particles within their structural framework. This

endeavour is optimally facilitated through microscopic techniques, potentially augmented by chemical point analysis [9].

As some authors recognise [9–11], instrumental bulk analyses such as X-ray diffraction or chemical analysis are less capable of tracing the binder constituents than imaging or microscopical analytical tools.

This study proves innovative as it combines elementary point chemical analyses with polarised light microscopy. It aims to group different mortar types according to their binders, distinguishing mortars made with hydraulic binders, namely 20th-century Portland cement, natural cement and NHL.

Since the main factors in obtaining the various types of mortar binders depend on the raw material and the temperature of calcination and/or sintering — the latter depending on the manufacturing technology available at the time — the applied methodology and the results obtained can be used to characterise mortars from other historical periods.

The aspects identified above are even more critical regarding material compatibility. It greatly impacts conservation and restoration interventions, which must respect the original materials' physical, mechanical, and chemical characteristics [12,13] as much as possible to prevent future decay phenomena.

2. Materials and Methods

2.1. Samples

Fifty-one samples were investigated from buildings constructed throughout the 20th century in Lisbon (Portugal), whose characteristics and sampling setup can be consulted elsewhere [14]. Additionally, two natural cement samples were analysed from cast decorative elements in Barcelona buildings (Spain), built between the end of the 19th century and the beginning of the 20th century [15].

Table 1 presents the type of binder and the binder to the aggregate ratio (b:a) of the analysed render and plaster samples and their construction or application period. The b:a was relevant to investigate if this ratio would impact the chemical analysis results.

For lime mortars, the b:a was calculated using the insoluble residue (IR) values obtained by wet chemical analysis and the CO₂ content obtained by thermogravimetry [14]. The insoluble residue (IR) corresponds to siliceous aggregate content. In contrast, the binder content was calculated from the CO₂ content converted to Ca(OH)₂ [16], considering that all of the CO₂ came from the decomposition of carbonated lime (CaCO₃). For ordinary cement mortars, the binder content was obtained according to the procedure described in [17]. The b:a was obtained by point counting in thin sections for mortars with carbonate aggregates, according to RILEM Technical Committee TC167-COM guidance [18].

The samples analysed have the following binders: air lime (AL), natural hydraulic lime (NHL), natural cement (NC), ordinary Portland cement (OPC), Portland composite cement with mineral additions, like fly ash (FA) or ground granulated blast furnace slags (GGBS), and blended air lime and Portland cement (with OPC or white Portland cement - WPC).

Table 1. Mortars from Lisbon (Portugal) and Barcelona (Spain) buildings.

Sample Id.	Construction period	Case study/Building	Binder type	Binder to aggregate ratio by weight (b:a)
CVT1B	1902–1903	CVT (1903)	AL	1:5.4
CVT1C			AL	1:7.8
CVT3B			AL	1:4.3
AR49-2B	1920–1923	AR49 (1923)	AL	(c)
AR49-6C			AL	1:5.8
AR49-7B			AL	1:3

Sample Id.	Construction period	Case study/Building	Binder type	Binder to aggregate ratio by weight (b:a)
AR49-8A			AL	1:2.9
AR49-8B			AL	1:11.2
AR49-11B			AL	1:6.7
AR49-15B			AL	1:7.1
AR49-15C			AL	1:7.9
IRF1B	1934–1938	IRF (1938)	AL+OPC	1:0.1: 7
IRF2A			AL	1:4.3
IRF2B			AL	1:9.9
IRF3A			AL	1:4.2
IRF3B			AL	1:8
IRF4A			AL+OPC	1:0.4:5.4
IRF7A			AL+OPC	1:0.4:3.8
IRF7B			AL+OPC	1:0.4:5.3
CBP1A	1938–1939	CBP (1939)	AL	1:8.4
CBP4B (d)			OPC	1:20.3
CBP6B			AL	1:8.7
CBP7B			AL	1:11.2
DN9A	1936–1940	DN (1940)	OPC	1:6.1
DN10A			OPC	1:7
DN11A			OPC	1:7.4
DN11B			OPC	1:4.2
DN12A			OPC	1:12.9
DN12B			AL+OPC	1:2.1:15.1
DN12C			OPC	1:4.2
DN12D			AL	1:4.3
DN19B			PCC	1:25.2 (a)
DN19C			OPC	1:8.9
DN19D			AL+PCC	1:1:6 (a)
AAC1A	1942–1944	AAC (1944)	AL+OPC	1:0.2:6.1
AAC1B			AL+OPC	1:0.2:7
AAC2A (c)			AL+WPC	1:0.3:1.0
AAC2B			OPC	1:24.5
AAC3A (c)			OPC	1:3.0
AAC4A (c)			OPC	1:1.9
LIP1A	1955–1957	LIP (1954)	OPC	1:7.6
LIP9A			OPC	1:6.6
EUA53-2A (c)	1966–1969	EUA53 (1970)	WPC (e)	1:3.7
EUA53-2B			OPC	1:6.7
EUA53-3A (c)			WPC (e)	1:19.1
EUA53-3B			OPC	1:4.9
EUA53-4A (c)			WPC	1:11.1
EUA53-4B			OPC	1:11.5
FCG4A	1963–1969	FCG (1975)	OPC	1:10.2
JRP2A	1984–1987	JRP (1987)	PCC	1:4.9 (a)

Sample Id.	Construction period	Case study/Building	Binder type	Binder to aggregate ratio by weight (b:a)
UNL3A	2000–2002	UNL (2002)	OPC	1:10.2
0-NC	1887	Hivernacle (Barcelona)	NC	(b)
1-NC	1900	Villarroel (Barcelona)	NC	(b)

¹ Legend: AL – air lime; OPC – ordinary Portland cement; WPC – white Portland cement; PCC – Portland composite cement; NC – natural cement; (a) – overestimated aggregate content, due to the presence of mineral additions (GGBS – samples DN19D and JRP2; FA – sample DN19D); (b) – not assessed; (c) – stone-imitating mortars; (d) – mortar with ceramic aggregates; (e) – stone imitating mortar with limestone filler

In addition, mortar specimens formulated in the laboratory were also analysed. Their formulations can be found in Table 2 [19–21].

Table 2. Composition of laboratory formulated mortar specimens.

Specimens ID	Mortar's formulation	Binder type	B:a (a)
CA-Sb-CP-360d	CL90-S air lime mortar with siliceous sand. 360 days laboratory curing	AL	1:11
CA-AL-CP-360d	CL90-S air lime mortar with washed siliceous sand. 360 days laboratory curing	AL	1:11
CH-AL-CP-360d	NHL 3.5 mortar with washed siliceous sand. 360 days laboratory curing	NHL	1:5.6
CH-Sb-CP-360d	NHL 3.5 mortar with siliceous sand. 360 days laboratory curing	NHL	1:5.6
CEM I (42.5)	Portland cement mortar (CEM I 42.5) with siliceous sand. 180 days laboratory curing	OPC	1:3
CEM I (52.5)	Portland cement type mortar (CEM I 52.5) with siliceous sand. 180 days laboratory curing	OPC	1:3
Li310-Ref-fib	Blended mortar with air lime and Portland cement (CEM I 42.5) with siliceous sand and organic fibres. 360 days laboratory curing	AL+OPC	1:2.6:26.3
Li310-Ref	Blended mortar with air lime and Portland cement (CEM I 42.5) with siliceous sand. 360 days laboratory curing	AL+OPC	1:2.6:26.3
CA-AL-CP-720d	CL90-S air lime mortar with washed siliceous sand. 720 days laboratory curing	AL	1:11
CH-AL-CP-720d	NHL 3.5 mortar with washed siliceous sand. 720 days laboratory curing	NHL	1:5.6
124A	Blended mortars with air lime and white Portland cement (CEM I 42.5) with siliceous sand. 4 years laboratory curing	AL+WPC	1:1.3:19.7
134A		AL+WPC	1:0.9:17.5

Legend: AL – air lime; OPC – ordinary Portland cement; WPC – white Portland cement; NHL – natural hydraulic lime; AL+OPC (or WPC) – blended air lime and ordinary Portland cement or white Portland cement; (a) – binder to aggregate ratio.

2.2. SEM-EDS and Principal Component Analysis

Scanning electron microscopy with energy dispersive X-ray spectrometry (SEM-EDS) was performed in a TESCAN MIRA 3 field emission microscope combined with a BRUKER XFlash 6|30 EDS system. Polished flat specimens or thin sections from each mortar sample and prepared as described in the following section were analysed in backscattered electron mode, with a chamber pressure of 20 Pa and 20 kV accelerating voltage, using a magnification over 500x in paste areas.

Over 50 EDS points were captured in each specimen, being the oxygen calculated by stoichiometry [22] and rejecting the values for Al/Si and Ca/Si atomic ratios higher than 10% of the coefficient of variation.

Principal Component Analysis (PCA) was performed using the results of the EDS analysis processed with OriginPro 9.0 software. PCA was performed to test and explore a mortar type's clustering structure to help understand how clusters are distributed and whether they are well-separated or overlapping.

2.3. Optical microscopy - Petrography

The thin section technique, a significant advancement in the field of petrography, was developed by 19th-century geologists. It initially aided in studying rocks and minerals, and its application later expanded to include construction materials like concrete and mortar by the 1920s [23]. Today, this versatile technique is widely employed across various materials, including brittle substances like concrete and mortar. The samples were stabilised through embedding in epoxy resin, enabling cutting and grinding to a final thickness of 20–30 μm .

Petrographic observations were then conducted on thin sections using an Olympus BX60 petrographic microscope featuring magnification lenses of 5x, 10x, 20x, and 40x. Residues within the mortar matrix necessitate microscopic tools to pinpoint the binder type [24], especially when distinguishing between the various hydraulic binders, which is why it became essential to apply this technique. It should be noted that petrography was only used to distinguish between mortars with hydraulic binders whenever the SEM-EDS methodology was inconclusive. Both methods (SEM-EDS and petrography) are complementary but should be used together.

3. Results and Discussion

3.1. SEM – EDS and Principal Component Analysis

EDS analysis and observations in backscattered mode were performed to mark out and group each type of binder used in terms of chemical composition. The analyses helped detect whether there were significant chemical differences between blended air lime-Portland cement mortars and the other mortar types, considering the variability of the mix-design properties that could influence the composition, namely the binder-to-aggregate ratio.

The chemical compositions obtained by EDS were used to calculate the Al/Ca and Si/Ca atomic ratios (Table 3).

The hydraulicity of binders is highly variable [25] and was first determined by Louis Vicat (1818) [26] using the Hydraulicity Index. Vicat synthesised the available knowledge and directly linked hydraulicity to the SiO_2 and Al_2O_3 content. Subsequently, Eckel (2005) [27] introduced a novel index known as the Cementation Index. This index incorporates the influence of Fe_2O_3 and MgO on hydraulicity, presuming that all available SiO_2 combines with CaO to produce C_3S (Ca_3SiO_5) and that all Al_2O_3 combines to produce C_3A ($\text{Ca}_3\text{Al}_2\text{O}_6$). MgO is equated with CaO and Fe_2O_3 with Al_2O_3 .

Nevertheless, this representation oversimplifies matters, as the mineralogy of hydraulic binders is more intricate than assumed [25]. The combustion temperature and duration indirectly influence the hydraulic characteristics, impacting the product's mineralogy [28]. Despite acknowledging this observation, the selection of Al/Ca and Si/Ca elemental atomic ratios is rationalised due to the importance of the $\text{CaO-SiO}_2\text{-Al}_2\text{O}_3$ system

in evaluating the hydraulicity of mortars and binders, as evidenced by Mertens et al., 2008 [29], who scrutinised the composition of historical calcareous hydraulic binders within that chemical system.

Table 3. Al/Ca and Si/Ca atomic ratios obtained by EDS of the mortars from the buildings analysed and of laboratory formulated test specimens.

Sample Id.	Case study	Binder type	Al/Ca	Si/Ca
CVT1B	CVT (1903)	AL	0.03	0.11
CVT1C		AL	0.06	0.19
CVT3B		AL	0.02	0.15
AR49-2B	AR49 (1923)	AL	0.05	0.13
AR49-6C		AL	0.05	0.12
AR49-7B		AL	0.02	0.10
AR49-8A		AL	0.03	0.11
AR49-8B		AL	0.05	0.19
AR49-11B		AL	0.07	0.16
AR49-15B		AL	0.05	0.14
AR49-15C		AL	0.05	0.17
IRF1B	Lisbon buildings	AL+OPC	0.12	0.28
IRF2A		AL	0.04	0.09
IRF2B		AL	0.04	0.12
IRF3A		AL	0.06	0.12
IRF3B		AL	0.05	0.14
IRF4A		AL+OPC	0.11	0.35
IRF7A		AL+OPC	0.13	0.32
IRF7B		AL+OPC	0.11	0.30
CBP1A	CBP (1939)	AL	0.07	0.20
CBP4B		OPC	0.23	0.44
CBP6B		AL	0.03	0.13
CBP7B		AL	0.09	0.21
DN9A	DN (1940)	OPC	0.11	0.39
DN10A		OPC	0.09	0.34
DN11A		OPC	0.10	0.40
DN11B		OPC	0.10	0.33
DN12A		OPC	0.12	0.44
DN12B		AL+OPC	0.13	0.32
DN12C		OPC	0.12	0.45
DN12D		AL	0.05	0.15
DN19B		PCC	0.23	0.41
DN19C		OPC	0.07	0.31
DN19D		AL+PCC	0.13	0.37
AAC1A	AAC (1944)	AL+OPC	0.05	0.24
AAC1B		AL+OPC	0.09	0.27
AAC2A		AL+WPC	0.05	0.22
AAC2B		OPC	0.09	0.36

Sample Id.	Case study	Binder type	Al/Ca	Si/Ca
AAC3A	LIP (1954)	OPC	0.10	0.31
AAC4A		OPC	0.09	0.34
LIP1A		OPC	0.13	0.35
LIP9A		OPC	0.07	0.32
EUA53-2A	EUA53 (1970)	WPC	0.05	0.22
EUA53-2B		OPC	0.09	0.30
EUA53-3A		WPC	0.03	0.21
EUA53-3B		OPC	0.08	0.32
EUA53-4A		WPC	0.08	0.30
EUA53-4B		OPC	0.09	0.32
FCG4A	FCG (1975)	OPC	0.11	0.33
JRP2A	JRP (1987)	PCC	0.17	0.49
UNL3A	UNL (2002)	OPC	0.08	0.27
CA-Sb-CP-360d	Laboratory formulated test specimens	AL	0.06	0.11
CA-AL-CP-360d		AL	0.05	0.07
CH-AL-CP-360d		NHL	0.15	0.26
CH-Sb-CP-360d		NHL	0.12	0.21
CEM I (42.5)		OPC	0.09	0.33
CEM I (52.5)		OPC	0.08	0.45
Li310-Ref-fib		AL+OPC	0.05	0.25
Li310-Ref		AL+OPC	0.05	0.27
CA-AL-CP-720d		AL	0.06	0.17
CH-AL-CP-720d		NHL	0.12	0.28
124A		AL+WPC	0.04	0.21
134A		AL+WPC	0.08	0.27
0-NC	Barcelona buildings	NC	0.12	0.23
1-NC		NC	0.16	0.35

Legend: AL – air lime; OPC – ordinary Portland cement; WPC – white Portland cement; PCC – Portland Composite Cement; AL+OPC (or WPC, or PCC) – blended air lime and Portland cement (for each type); NHL – Natural hydraulic lime; NC – Natural cement

Figure 1 shows an expected increase in hydraulic binders' Si/Ca ratio, while the Al/Ca ratio is variable within the specified clusters. Although there are few laboratory test specimens, finding a chemical composition concordance between them and the other analysed samples is possible. The only discrepancy found is the composition of the mixed mortars, which has such a dispersion that some compositions are encompassed in the cluster of cement mortars or even at the limit between natural cement and NHL mortars.

The presence of limestone filler in the paste of stone-imitating mortars reduced both ratios, as can be seen in cluster E1. Cluster E2 stands out from the others as it includes binders with mineral or pozzolanic additions rich in silica or alumina.

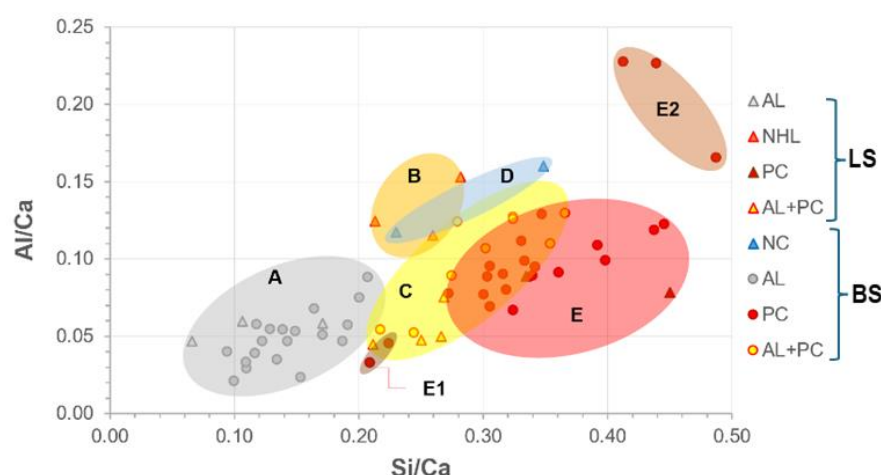


Figure 1. Si/Ca vs. Al/Ca plot of laboratory test specimens (LS) and building samples (BS) with clustering. Group A: Air Lime mortars (AL); group B: NHL mortars (B); group C: Blended air lime-Portland cement mortars (AL+PC); Group D: Natural cement mortars (NC); group E: Portland cement mortars (PC); sub-group E1: Portland cement stone imitating mortars with limestone filler; sub-group E2: Portland cement mortars with mineral additions or with pozzolanic additives. PC includes all types of Portland cement.

For comparative purposes and to attempt to improve the discrimination of this group of samples, the Principal Component Analysis (Figure 2) was carried out considering the analytical results presented in Table 3. The by-mixed mortars have high dispersion, and their cluster overlaps with the PC cluster. However, the air-lime and Portland cement mortars were distinctively separated. A plot in the plane of the two principal components (PC1 and PC2) is shown in Figure 3. PC1 explains 43.73% of the variation and is controlled in the positive sense primarily by the contents in O, Si, Al and Fe (somehow related to hydraulicity, which depends primarily on the clay content of the raw material) and in the opposite sense by the content in Ca (air-lime binder's main element) and Cl. PC2 explains 16.38% of the variation and is controlled in the positive sense primarily by the contents in Ca and Na; in the opposite sense, no element has influence (as seen in the loadings plot of Figure 3). Although Cl may derive from the composition of the epoxy resin, which is cannot be proved for all the analysed samples, the influence of Na (PC2) raises questions regarding the contamination by salts and their possible influence on the analytical results of the binders. XRD detected Halite (NaCl) in samples CVT1C, CVT3B, AR49-7B and AR49-11B [14], though only AR49-7B and AR49-11B are influenced by both contents. Nonetheless, sodium may be derived from the sodium-feldspars (i.e., albite) from the aggregates, as the same authors stated elsewhere [14].

Similarly to Figure 1, Figure 2 shows a cluster (E1) of samples with mineral additions and pozzolanic materials and another, cluster E2, which refers to stone imitating mortars with limestone filler. As an outlier, sample CBP7B has a high influence of sulphur derived from gypsum in the binder [14]. Figure 4 shows a detail of the binder paste of this sample confirming the presence of gypsum (needle-shaped crystals), where it can be seen the distribution of the elements Ca and S. This sample stands out from the others since it is a supporting mortar of a crown moulding plaster element [14]. The incorporation of gypsum must, therefore, be related to the construction technique.

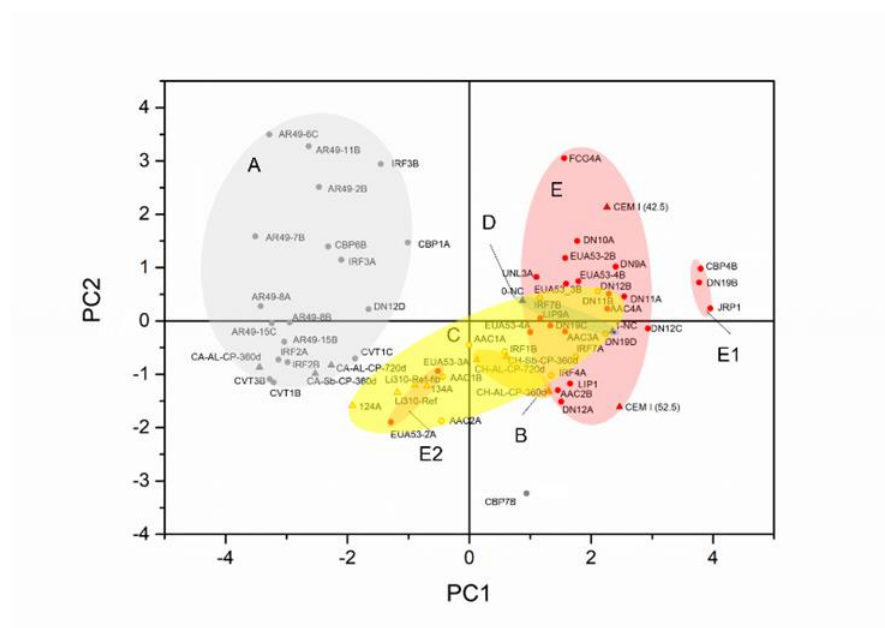


Figure 2. Score plot of the PCA of the analysed samples, including the laboratory test specimens. Legend: Group A: Air Lime mortars (AL); group B: NHL mortars (B); group C: Blended air-lime with Portland Cement mortars (AL+PC); Group D: Natural cement mortars (NC); group E: Portland cement mortars (PC); sub-group E1: Portland cement stone imitating mortars with limestone filler; sub-group E2: Portland cement mortars with mineral additions or with pozzolanic potential. PC includes all types of Portland cement.

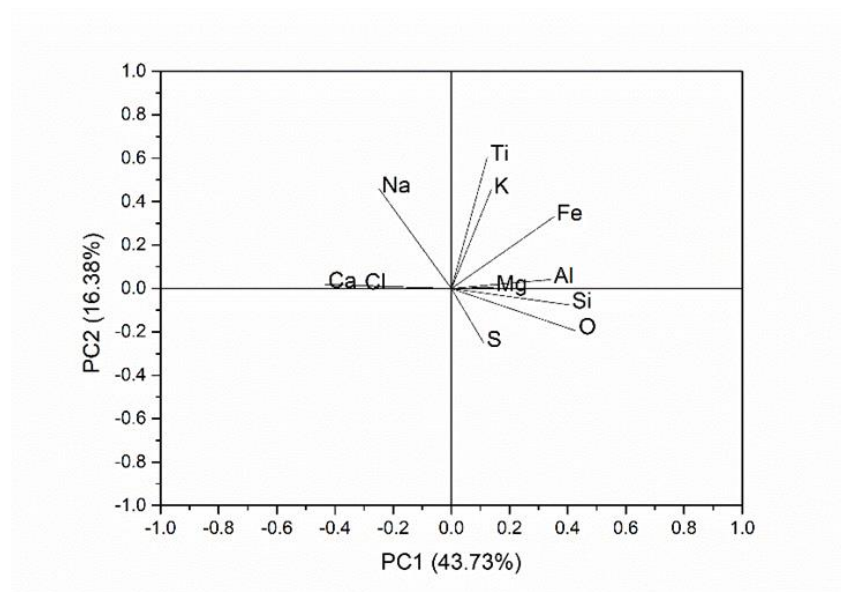


Figure 3. Loadings plot of the PCA of the experimental and the laboratory test specimens.

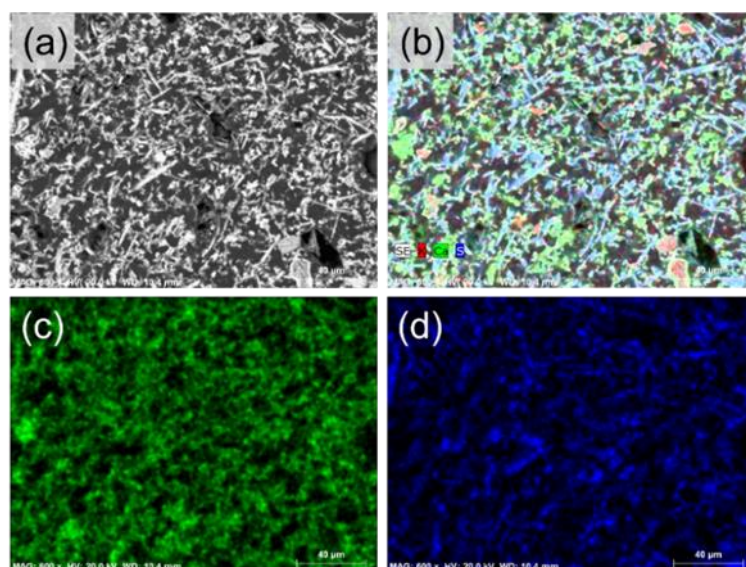


Figure 4. Backscattered scanning electron images of the binder of the sample CBP7B. Needle-shape gypsum crystals forming a loose-like binder network (a); X-ray map of elements K, Ca, and S (b); X-ray maps of elements Ca (c) and S (d).

According to the EDS results (see Figures 1 and 2), mortars in which lime has been mixed with Portland cement are chemically similar to cement mortars. The plot in Figure 5 shows no tendency for the Si/Ca ratio to increase as the binder content (in this case, Portland cement) increases. This finding has significant implications, as it suggests that the Portland cement content in the mix does not influence considerably the chemistry of the paste, which can be explained by the fact that the pastes were poorly mixed or there may be an influence from the composition of the raw materials from different origins to contribute to this compositional variability.

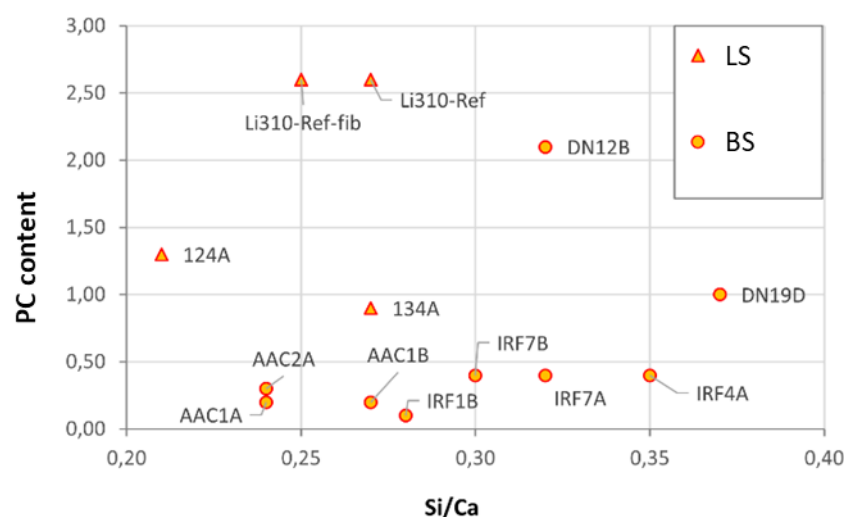


Figure 5. Si/Ca to Portland cement content (from b:a ratio) in the lime-mixed Portland cement mortars. Legend: LS – laboratory mortar specimens; BS – building mortar samples.

3.2. Optical microscopy – Petrography

Considering the elemental analysis results, more specifically the Si/Ca ratio vs. Al/Ca ratio, there is a noticeable overlap between groups B (NHL mortars) and D (Natural cement mortars) and between C (Blended air lime-Portland cement mortars), E (Portland

cement mortars) and E1 (Portland cement stone imitating mortars with limestone filler), a complementary approach is needed to identify the binders unequivocally. A literature review shows that each type of binder has its characteristics with its compounds. Much of the identification using optical microscopy is carried out to find residues resulting from the manufacturing process, i.e., ‘fossil’ traces of the raw material, residues (or ‘relicts’) of the binder that have not produced chemical and physical reactions, or even neoformation products resulting from interaction with the binder matrix.

Air lime, which has been extensively studied, is often characterised by the presence of lumps. Lime lumps are fragments macroscopically showing a whitish colour and sometimes an inconsistent appearance [30–33]. Among several authors, Cantisani et al. 2022 [32], observing the thin section of lumps under a polarised light microscope, stated that the presence of lime lumps is fundamental to recognise the lime binder nature, allowing information about the stone used to produce lime. According to Pavia & Caro (2007) [34], binder properties, including reactivity, shrinkage, cohesion and fineness, can also be analysed with petrographic microscopy, providing essential clues on lime calcination and slaking. The same authors point out that the accumulation of lime lumps often appears fractured under the microscope because pure calcium lime is a non-hydraulic binder with a high retraction coefficient. Other authors state that the presence of lime lumps can indicate incomplete calcination [35], poor mixing [36], or the practice of “hot lime mixing” [37] when they are abundant. Regarding the mortars in this study, particularly those from the Lisbon buildings, the lime binders are clearly identified by the presence of the lime lumps, as shown in Figure 6. In the case of blended binders, i.e., Portland cement with a lime mixture, the identification of lime lumps also makes it possible to conclude that lime was used in the mortar formulation (Figure 9b).

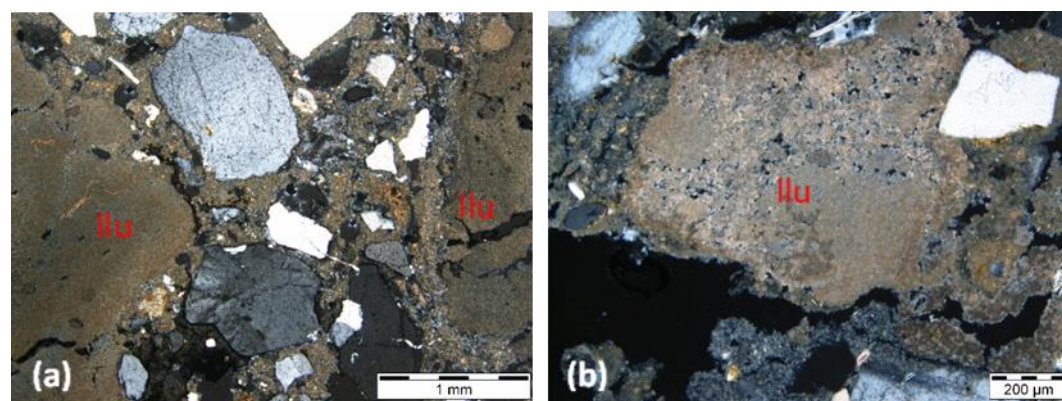


Figure 6. AR49-6C (a) and IRF2B (b) thin section micrographs in transmitted cross-polarised light showing lime lumps (llu).

When employing appropriate petrographic techniques, there is minimal risk of confusing a lime with Portland cement. Therefore, we can confine ourselves to the differences between the various types of hydraulic binders, as they present chemical overlaps in the elemental relationships studied and recognised by other features.

Whether in hot-mixed lime, fat lime putty, or eminently hydraulic lime, the essential constituent of the raw material remains calcium hydroxide. The manufacturing procedures involved are notably distinct from those of Portland cement. A limestone of varying purity undergoes a process known as “calcination,” which is heated to a temperature sufficient to expel the carbon dioxide in the original limestone. This temperature threshold is significantly below the clinkering point, usually below 1000 °C. The primary output is calcium oxide or free lime; however, this compound is unstable, necessitating an additional step known as slaking [24].

The most eminent difficulty is the differentiation between NHL, natural cement, and air lime mixed with materials that promote hydraulicity, such as natural or artificial pozzolans. That difficulty is due to several factors, such as the optical similarity between natural cement and natural hydraulic lime. As far as natural cements are concerned, the poor quality of the milling technology means that the calcined marl fragments remain unhydrated during the setting process, making it easier to identify unhydrated belite crystals inside the lumps [15].

Table 4 compiles some key compounds according to several authors, and it is intended to be a guide for identifying the hydraulic binders from the compounds observed. Given the affinity between the NHL binder and the hydraulic mortars, both materials are combined in the exact identification batch. Despite using a transmitted light microscope, it should be kept in mind that using reflected (incident) light is beneficial for observing some of these components. Incident light microscopy proves helpful for mortars containing Portland cement (Figure 8), while polarised microscopy in transmitted light is advantageous for all types of hydraulic mortars [9].

Figures 7 to 9 show some key characteristics described in Table 4 and found in the samples studied, except the NHL mortar samples due to the inexistence of thin sections. The images show the presence of compounds that indicate different types of hydraulicity according to the binder used.

Table 4. Main characteristics for identifying binders by optical microscopy according to several authors

		Authors [by reference]						
NHL and other Hydraulic lime mortars/binders	[10]		[24]	[38]	[39]	[40,41]	[40,42,43]	[48]
	Large C2S and C3S phases in a small amount of a brown matrix consisting of C3A and C4AF		Small clusters of C2S may be detected in trace quantities in hydraulic limes	Dominant C2S grains can present striations in different directions	Presence of “hot spots” as part of the hydraulic phases that result from local higher temperatures in the lime kiln.	If reaction rims did not develop, hydraulic phases dispersed in the binder can nevertheless still be observed both as veins and as pore filling.	Presence of small dark inclusions (non-hydrated relicts of C2S) that can be easily recognised.	C3S can be formed due to an overheating of the raw materials during the production of NHL
			C3S can also be present in smaller quantities	Hydration rims can be observed around individual hydraulic phases as a colourless rim	The presence of gehlenite is a valuable indicator of the distinction between cement and natural hydraulic lime.		C2S: dark brown crystals medium-high relief, shaded contours, and sub idiomorphic habit.	
Natural Cement	[9]		[15]		[24]		[44]	[49]
	The NC residual nodules exhibit strong zoning which is best visible in transmitted light with parallel polars.		Presence of lumps of calcined marls in the natural cement (due to the calcination and to the deficient milling technology).		Under polarised light, the matrix of natural cements often appears spotted with dark isotropic areas broken by bright but dense carbonated regions.		High proportion of non-reactive ‘nodules’ or relicts (under-burned, well burned and over-burned).	Under-burned, well burned and over-burned marl fragments.
	NC mortars can be identified equally well at low magnifications as their binders contain residual compounds that are larger than the clinker of historic Portland Cement		Presence of unhydrated C2S crystals		The dispersed quartz grains and other sand-sized silicate minerals also aid in distinguishing natural cements. These tend to retain most of their original texture when burned at calcining temperatures.		The largest ‘nodules’ are of millimetre size	NHL do not show calcined marl fragments and have a more homogeneous structure.

Authors [by reference]			
	Absence of unhydrated C3S crystals	Contain greater percentage of relicts than either the hydraulic limes or the Portland cements	Lime nodules can be observed in the NHL samples, while the natural cements lack these nodules.
	[15]	[24]	[45–47]
OPC	Large size of the unhydrated C3S crystals in historic Portland cements. The calcination process in vertical kilns was longer than in a modern horizontal kiln and it allowed the C2S and C3S crystals to acquire a larger size than in modern Portland cement.	Portland cement pastes are homogeneously isotropic or dark-colored where cementitious gels have formed, broken only by thin dispersed grains of calcium hydroxide which appear bright-colored.	The unhydrated cement grains are identified by the optical properties of the cement minerals, primarily C3S and C2S
WPC	[24] The C2S phases are not surrounded by a brown-colored crystallographically indistinct ferrite phase (absence of brownish C4AF in the residual cement grains)		
PCC	[45,46] Unhydrated fly ash particles; GBFS - glassy slag particles with reddish hydration rims.		

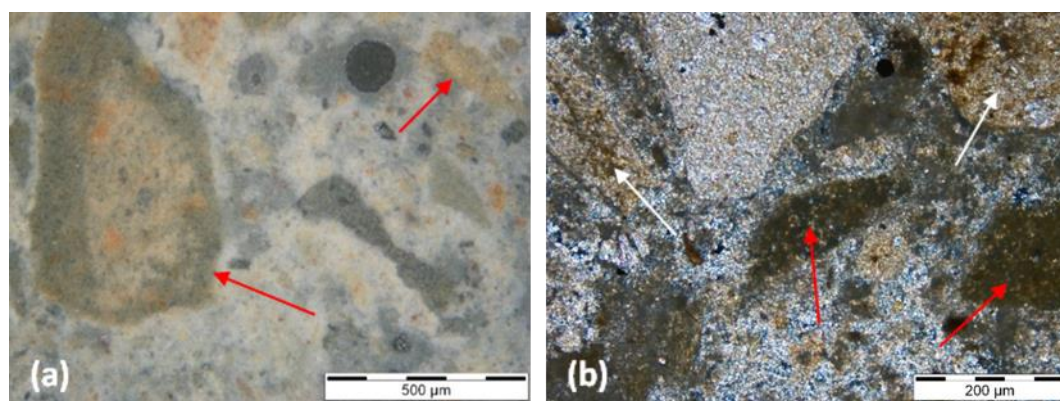


Figure 7. 0-NC thin section micrographs. Legend: (a) - Fragments of calcined marl from the natural cement sample in incident light, dark field. These fragments are characterised by a hydrated outer ring (red arrows). (b) - detail of marls with non-hydrated belite inside lumps (red arrows); residual, under-burned relicts exhibiting low reactivity (white arrows) and the original rock texture observed in transmitted cross-polarised light.

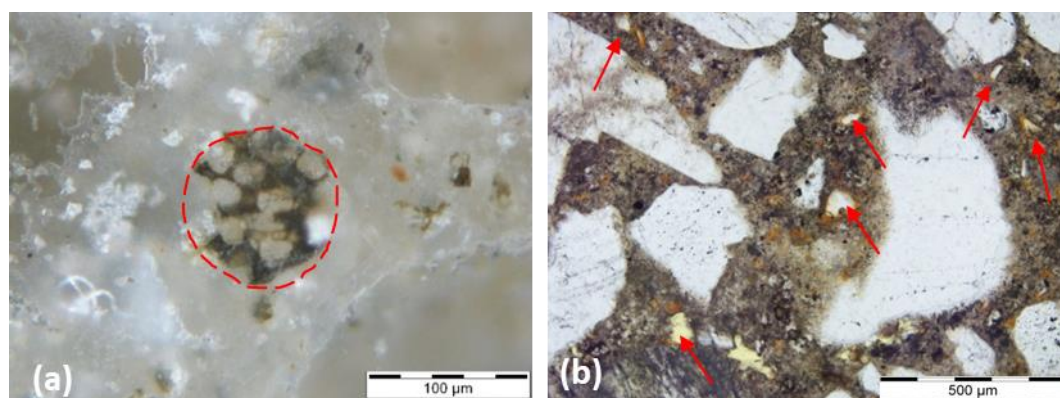


Figure 8. Polished section micrograph of Li310-Ref test specimen in incident light, dark field (a), and thin section micrograph of JRP2A sample in transmitted plane polarised light (b). Legend: unhydrated Portland cement clinker grain (red dotted circle) containing C₃S (elongated), C₂S (rounded crystals) and a brownish phase corresponding to C₄AF; GBFS grains in a Portland cement matrix, showing typical orange to red hydration rims (red arrows).

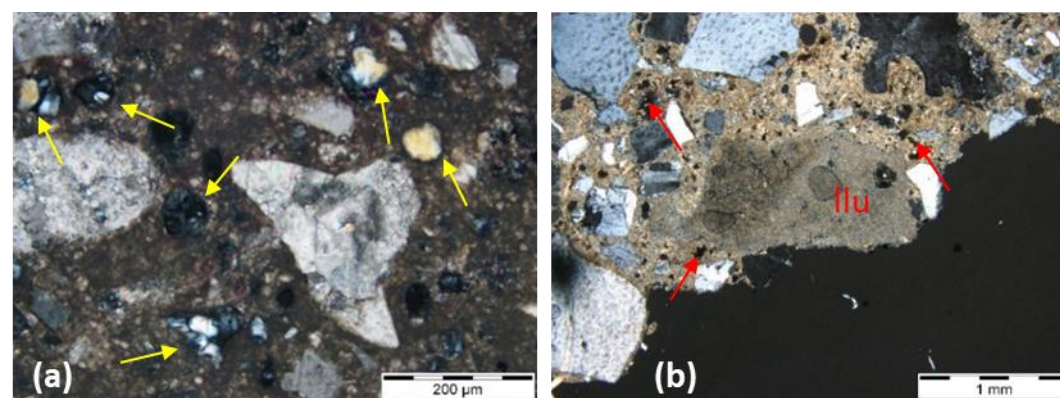


Figure 9. Thin-section micrograph of EUA53-4A in transmitted cross-polarised light (a), and thin section micrograph of IRF4A in transmitted cross-polarised light (b). Legend: unhydrated white Portland cement clinker grains (yellow arrows) showing no C₄AF phase in the residual cement grains; lime lump (llu) and Portland cement clinker grains (red arrows) coexisting in the same sample, indicating air lime with mixed ordinary Portland cement as binders

4. Conclusions

The main conclusions of this work are:

- Analytical systematisation for the identification of binders in historic mortars should consider a workflow that begins with preparing samples to obtain polished surfaces and thin sections, then a combined approach applying EDS micro-analyses to the mortar pastes combined with optical microscopy to identify the binder types accurately.
- The interval ranges for the chemical compositions of the binders were obtained with precision through EDS analyses. The following interval of elemental ratios Al/Ca and Si/Ca were established for the types of binders identified in Table 5, ensuring the accuracy of the results.

Table 5. Ranges for chemical composition ratios (Al/Ca and Si/Ca) of binders

Binder type	Al/Ca		Si/Ca	
	Min.	Max.	Min.	Max.
Air Lime	0.02	0.09	0.09	0.20
Natural Hydraulic Lime	0.12	0.15	0.21	0.28
Natural Cement	0.12	0.16	0.23	0.35
Blended air lime and Portland cement (including ordinary, white and Portland composite cement types)	0.04	0.13	0.21	0.37
Portland Cement, (including ordinary and white types)	0.03	0.23	0.21	0.45
Portland composite cements	0.17	0.23	0.41	0.49

- When doubts persist about the samples’ hydraulicity, petrographic techniques must be applied parallel to EDS analytical work.
- When dealing with overlapping grouped chemical results, optical microscopy is a key step in identifying the key compounds of the binder. When consistently applied by a skilled petrographer, this practice ensures the accuracy and reliability of the results.
- In blended mortars, the pastes’ homogeneity, or compositional variability, which may be attributable to the influence of the raw materials’ composition, varying according to their provenance, points to being influential in EDS analyses.
- Although some of the samples analysed were manufactured in the laboratory, namely the natural hydraulic lime, Portland cement and air lime mixed with Portland cement test specimens, the chemical results can be extrapolated to these types of binders, historically applied in other periods, since the raw materials and calcination temperatures are similar to those obtained in the past, even though today there is greater quality control in the manufacturing processes.

Author Contributions: Conceptualization, L.A., and A.S.S.; methodology, L.A. and A.S.S.; software, L.A; validation, A.S.S., R.V. and J.M.; investigation, L.A., A.S.S., R.V., J.M.; writing—original draft preparation, L.A.; writing—review and editing, L.A., A.S.S., R.V., and J.M.; supervision, A.S.S., R.V., and J.M. All authors have read and agreed to the published version of the manuscript.

Funding: This research was funded by the Portuguese Foundation for Science and Technology — Fundação para a Ciência e a Tecnologia — FCT, grant SFRH/BD/112809/2015.

Data Availability Statement: No new data were created.

Acknowledgments: The authors would like to acknowledge FCT through PO-CI-01-0145-FEDER-031612 research project: CEMRESTORE: Mortars for early 20th century buildings' conservation: compatibility and sustainability and the collaborative researcher Judith Ramirez-Casas for making available thin sections of natural cement mortars from the Barcelona buildings. The authors would like to thank researcher Sílvia Pereira for her support in software computing. The authors also acknowledge the buildings' owners for study authorisations and the National Laboratory for Civil Engineering for its support through the projects DUR-HERITAGE—Durability and characterisation of historical interest construction materials and PRESERVE—Preservation of renders from built heritage with cultural value: identification of risks and contribution of traditional knowledge and new materials for conservation and protection.

Conflicts of Interest: The authors declare no conflicts of interest.

References

1. Elsen, J.; Van Balen, K.; Mertens, G. Hydraulicity in historic mortars: a review. In Proceedings of the 2nd Historic Mortars Conference HMC2010 and RILEM TC 203-RHM Final Workshop, Prague, Czech Republic 22-24 September, 2010.
2. Furlan, V.; Bissenger, P. Les mortiers anciens. Histoire et essai d'analyse scientifique *Reveu Suisse d'art et d'Archéologie* **1975**, *32*, 2-14.
3. Rispoli, C.; Montesano, G.; Verde, M.; Balassone, G.; Columbu, S.; De Bonis, A.; Di Benedetto, C.; D'Uva, F.; Esposito, R.; Graziano, S. F.; Mercurio, M.; Morra, V.; Cappelletti, P. The key to ancient Roman mortars hydraulicity: ceramic fragments or volcanic materials? A lesson from the Phlegrean archaeological area (southern Italy). *Const. Build. Mater.* **2024**, *411*, 134408, <https://doi.org/10.1016/j.conbuildmat.2023.134408>.
4. Parker, J. A certain cement or terras to be used in aquatic and other buildings and stucco Work. *British Patent n. 2120*, 27 July, 1796.
5. Kozłowski, R.; Hughes, D.; Weber, J. Roman cements: key materials of the built heritage of the 19th Century. In *Materials, Technologies and Practice in Historic Heritage Structures*; Dan, M.B., Přikryl, R., Török, Eds.; Springer, Dordrecht, The Netherlands, 2010. https://doi.org/10.1007/978-90-481-2684-2_14
6. CEN EN 459-1. Building lime – Part 1: Definitions, specifications, and conformity criteria. *European Committee for Standardization*, Brussels, 2015.
7. Coutinho, A. S. *Fabrico e propriedades do betão*; Volume I, Laboratório Nacional de Engenharia Civil (LNEC), Lisboa, Portugal, 1988.
8. Hughes, D.; Swann, S.; Gardner, A. Roman cement. *Journ. Archit. Conserv.* **2007**, *13*:1, 21-36, DOI: 10.1080/13556207.2007.10784986
9. Weber, J.; Köberle, T.; Pintér, F. (2019). Methods of microscopy to identify and characterise hydraulic binders in historic mortars—A methodological approach. In *Historic Mortars*; Hughes, J., Válek, J., Groot, C., Eds.; Springer, 2019. https://doi.org/10.1007/978-3-319-91606-4_2
10. Callebaut, K.; J. Elsen; Van Balen, K.; Viaene, W. Nineteenth century hydraulic restoration mortars in the Saint Michael's Church (Leuven, Belgium): Natural hydraulic lime or cement? *Cem. Concr. Resear.* **2001**, *31* (3), 397–403. doi:10.1016/S0008-8846(00)00499-3.
11. Gadermayr, N.; Pintér, F.; Weber, J. Identification of 19th century roman cements by the phase composition of clinker residues in historic mortars. In Proceedings of the 12th International Congress on the Deterioration and Conservation of Stone. New York, USA, 22-25 October 2012.
12. Veiga, M.R.; Aguiar, J.; Santos Silva, A., Carvalho, F. *Conservação e renovação de revestimentos de paredes de edifícios antigos*, LNEC, Lisboa, Portugal, 2004, p 126.
13. Veiga, M.; Velosa, A.; Magalhães, A. Evaluation of mechanical compatibility of renders to apply on old walls based on a restrained shrinkage test. *Mater. Struct.* **2006**, *40*(10), 1115-1126
14. Almeida, L.; Santos Silva, A.; Veiga, R.; Mirão, J. Composition of renders and plasters of award-winning buildings in Lisbon (Portugal): A contribution to the knowledge of binders used in the 20th Century, *Intern. Journ. Archit. Herit.* **2023**, DOI: 10.1080/15583058.2023.2242820
15. Mayo, C. M.; Ramírez-Casas, J.; Sanz, D.; Ezquerro, A. N.; Rosel, J. R. Methodology of identification of natural and historic Portland cements. Application and study in mortars of Madrid and Barcelona. In RILEM Proceedings Pro 130 of the 5th Historic Mortars Conference, Pamplona, Spain, 2019.
16. Middendorf, B.; Hughes, J. J.; Callebaut, K.; Baronio, G.; Papayianni, I. Investigative methods for the characterisation of historic mortars—Part 2: Chemical characterisation. *Mater. Struct.* **2005**, *38* (8), 771–80. doi:10.1007/BF02479290.
17. Arliguie, G.; Hornain, H. *Grandubé: Grandeurs associées à la durabilité des bétons*. 1st ed.; Presses Ecole Nationale Ponts Chaussees, Paris, France, 2007, p. 438.
18. Lindqvist, J.E.; Sandström, M. Quantitative analysis of historical mortars using optical microscopy. Characterisation of old mortars. *Mater. Struct., RILEM TC*. 2000; 167 (33), RILEM, Paris, France, doi:10.1007/BF02480600.
19. Santos, A.R., Veiga, M.R., Santos Silva, A., Brito, J., Álvarez, J.I. Evolution of the microstructure of lime based mortars and influence on the mechanical behaviour: The role of the aggregates. *Constr. Build. Mater.* 2018. Volume 187, pp. 907-922, <https://doi.org/10.1016/j.conbuildmat.2018.07.223>.

20. Santos, A.R.; Veiga, M.R.; Santos Silva, A.; Brito, J. 2019. Impact of aggregates on fresh mortars' properties. In Proceedings of 5th Historic Mortars Conference, Pamplona, Spain, 19-21 June 2019
21. Pederneiras, C.M. Improving cracking performance of mortars with selected recycled fibres for non-structural uses. PhD thesis in Civil Engineering, University of Lisbon, Instituto Superior Técnico, Lisbon, 2021.
22. Famya, C.; Brough, A. R.; Taylor, H.F.W. The C-S-H gel of Portland cement mortars: Part I. The interpretation of energy-dispersive X-ray microanalyses from scanning electron microscopy, with some observations on C-S-H, AFm and Aft phase compositions. *Cem. Concr. Resear.* **2003**, *3*, pp. 1389–1398.
23. Balksten, K.; Nitz, B.; Hughes, J.J.; Lindqvist, J.E. Petrography of historic mortar materials: polarising light microscopy as a method for characterising lime-based mortars. In Proceedings of the 5th Historic Mortars Conference, Universidad de Navarra, Pamplona, Spain, 19-21 June 2019.
24. Walsh, J. J. Petrography: Distinguishing Natural Cement from Other Binders in Historical Masonry Construction Using Forensic Microscopy Techniques. *Journ. ASTM Intern.* **2007**, Vol. 4, 1.
25. Elsen, J.; Mertens, G.; Snellings, R. Portland cement and other calcareous hydraulic binders: History, production and mineralogy. *Europ. Mineral. Uni. Notes in Mineral.* **2011**. Vol. 9, pp. 441-479. 10.1180/EMU-notes.9.11.
26. Vicat, L.J. *Recherches expérimentales sur les chaux de construction, les bétons et les mortiers ordinaires*. Goujon, Paris, France, 1818.
27. Eckel, E. Cements, limes and plasters. A facsimile of the 3rd ed. (1928). Donhead Publishing Ltd., 2005.
28. Mertens, G.; Elsen, J.; Laduron, D.; Brulet, R. Mineralogy of the calcium-silicate phases present in ancient mortars from Tournai. *Archéom.* **2006**, Vol. 30, 61-65.
29. Mertens, G.; Lindqvist, J.E.; Sommain, D.; Elsen, J. Calcareous Hydraulic Binders from a Historical Perspective. In Proceedings of the 1st Historical Mortars Conference, Characterization, Diagnosis, Conservation, Repair and Compatibility. Lisbon, Portugal, 1-15, 2008.
30. Pecchioni, E.; Fratini, F.; Cantisani, E. *Atlas of the Ancient Mortars in Thin Section under Optical Microscope*, 2nd ed.; Nardini: Florence, Italy, 2020; p. 78.
31. Bugini, R.; Toniolo, L. (1990). La presenza di grumi bianchi nelle malte antiche: Ipotesi sull'origine. *Arkos* 1990, 12, 4–8
32. Cantisani, E.; Fratini, F.; Pecchioni, E. Optical and Electronic Microscope for Minero-Petrographic and Microchemical Studies of Lime Binders of Ancient Mortars. *Minerals* **2022**, 12, 41. <https://doi.org/10.3390/min12010041>
33. Hughes J.; Cuthbert S. The petrography and microstructure of medieval lime mortars from the west of Scotland: Implications for the formulation of repair and replacement mortars. *Mater. Struct.* **2000**, Vol. 33, pp 594-600.
34. Pavia, S.; Caro, S. Petrographic microscope investigation of mortar and ceramic technologies for the conservation of the built heritage. In Proceedings of SPIE, Vol. 6618, Optics for Arts, Architecture, and Archaeology, Munich, July 2007.
35. Pavia, S.; Fitzgerald, B.; Howard, R. Evaluation of properties of magnesian lime mortar. In *Structural studies, repair, and maintenance of heritage architecture IX*; Brebbia C.A., Torpiano A. eds. Vol. 83. Transactions on the Built Environment, WIT Press, 2005, pp. 375-384.
36. Leslie, A. B.; Hughes, J. J. Binder microstructure in lime mortars: implications for the interpretation of analysis results. *Quarter. Journ. Engin. Geol.* **2002**, 35, 257-263.
37. Leslie, A. B.; Gibbons, P. Mortar analysis and repair specification. In Proceedings of International RILEM workshop on historic mortars: characteristics and tests. Bartos, Groot and Hughes eds. RILEM, 2000, pp. 273-280.
38. Furlan, V.; Pancella, R. Examen microscopique en lumière réfléchie de ciments, bétons et mortiers, Chantiers/Suisse, 1982, 13 (11), pp. 25 - 30.
39. Gödicke-Dettmering, T.; Strübel, G. Mineralogische und technologische Eigenschaften von hydraulischen Kalken als Bindemittel für Restaurierungsmörtel in der Denkmalpflege, *Giessener Geol. Schr.* **1996**, 56, pp. 131 - 154.
40. Pecchioni, E.; Fratini, F.; Cantisani, C. (2018) *Le Malte Antiche e Moderne tra Tradizione e Innovazione*, 2nd ed.; Pàtron: Bologna, Italy; pp. 231.
41. Moropoulou, A.; Cakmak, A.S.; Biscontin, G.; Bakolas, A.; Zendri, E. Advanced Byzantine cement based composites resisting earthquake stress: The crushed brick/lime mortars of Justinian's Hagia Sophia. *Constr. Build. Mater.* **2002**, 16, 543–552.
42. Pecchioni, E.; Fratini, F.; Cantisani, E. *Atlas of the Ancient Mortars in Thin Section under Optical Microscope*, 2nd ed.; Nardini: Florence, Italy; 2020, p. 78
43. Ingham, J. *Geomaterials under the Microscope: A Colour Guide*; John Wiley & Sons: Hoboken, NJ, USA, 2010, p. 192.
44. Hughes, D.; Swann S.; Gardner, A. Roman Cement, *Journ. Archit. Conserv.* **2007**, 13:1, 21-36, DOI: 10.1080/13556207.2007.10784986
45. Jepsen, B.B.; Christensen, P. Petrographic examination of hardened concrete. *Bull. Intern. Assoc. Engin. Geol.* **1989**, 39.
46. Poole, A.; Sims, I. *Concrete Petrography. A Handbook of Investigative Techniques*, 2nd ed; CRC Press, 2020.
47. Pavia, S. A Petrographic study of the technology of hydraulic mortars at masonry bridges, harbours and mill ponds. In Proceedings of Concrete Research and Bridge Infrastructure Symposium, 2008, pp. 253-264.
48. Klenner, J.; Meintrup, E.; Rother, W. Brennen von hydraulischem Kalk im Schwebegas-Calculator, *Zem.-Kalk-Gips* **1980**, 33 (10), pp. 498 - 504.
49. Mayo, C.; Sanz, D.; Pineda, J. I. (2018). Metodología simplificada de identificación mediante MOP de las cales hidráulicas y los cementos naturales. In proceedings of Tradición, versatilidad e innovación en la cal: un material de excelencia. In Proceedings of VI Jornadas FICAL – Forum Iberico de la Cal. Pamplona, 28-30 may 2018.